Research Article

Jiawen Wang[#], Ye Sun[#], Xuemei Zhao, Lin Chen, Shuyi Peng, Chunxin Ma*, Gaigai Duan, Zhenzhong Liu*, Hui Wang, Yihui Yuan, and Ning Wang*

A poly(amidoxime)-modified MOF macroporous membrane for high-efficient uranium extraction from seawater

https://doi.org/10.1515/epoly-2022-0038
received February 19, 2022; accepted March 18, 2022

Abstract: Although metal–organic frameworks (MOFs) own excellent uranium adsorption capacity but are still difficult to conveniently extract uranium from seawater due to the discrete powder state. In this study, a new MOF-based macroporous membrane has been explored, which can high-efficiently extract uranium through continuously filtering seawater. Through modifying the UiO-66 with poly(amidoxime) (PAO), it can disperse well in a *N*,*N*-dimethylformamide solution of graphene oxide and cotton fibers. Then, the as-prepared super-hydrophilic MOF-based macroporous membrane can be fabricated after simple suction filtration. Compared with nonmodified MOFs, this UiO-66@PAO can be dispersed uniformly in the membrane because it can stabilize well in the solution, which have largely enhanced uranium adsorbing capacity owing to the modified PAO. Last but not least, different from powder MOFs, this UiO-66@PAO membrane provides the convenient and continuously uranium adsorbing process. As a consequence, the uranium extraction capacity of this membrane can reach 579 $mg \cdot g^{-1}$ in 32 ppm U-added simulated seawater for only 24 h. Most importantly, this UiO-66@PAO membrane (100 mg) can remove 80.6% uranyl ions from 5 L seawater after 50 filtering cycles. This study provides a universal method to design and fabricate a new MOF-based adsorbent for high-efficient uranium recovery from seawater.

Keywords: uranium recovery from seawater, metal–organic frameworks, poly(amidoxime), graphene oxide, composite porous membrane

1 Introduction

Owing to the increasing global energy consumption, nuclear energy in the energy structure is constantly improving. Uranium has received widespread attention as the most important element in nuclear industry (1). The uranium resources deposit in seawater is 1,000 times than that on land, which can meet the need of mankind for thousands of years (2). The technology of uranium extraction from seawater will support the global economic development, particularly low-carbon nuclear power generation investment and exploitation. At present, a lot of strategies have been developed for uranium recovery, e.g., electrochemical deposition (3,4), ion-exchanging (5–8), liquid-extracting separation (9,10), bio-separation (11–14), and adsorption method (15–19). Among them, the adsorption method with the characteristics of simple, variable, and low cost is becoming one of the most promising and practicable methods (20–24).

# These authors contributed equally to this work.

*** Corresponding author: Chunxin Ma,** State Key Laboratory of Marine Resource Utilization in South China Sea, Hainan University, Haikou 570228, China; Research Institute of Zhejiang University-Taizhou, Taizhou 318000, China, e-mail: machunxin@hainanu.edu.cn
*** Corresponding author: Zhenzhong Liu,** Research Institute of Zhejiang University-Taizhou, Taizhou 318000, China, e-mail: zzliu@zju.edu.cn
*** Corresponding author: Ning Wang,** State Key Laboratory of Marine Resource Utilization in South China Sea, Hainan University, Haikou 570228, China, e-mail: wangn02@foxmail.com
Jiawen Wang, Ye Sun, Xuemei Zhao, Lin Chen, Shuyi Peng, Hui Wang, Yihui Yuan: State Key Laboratory of Marine Resource Utilization in South China Sea, Hainan University, Haikou 570228, China
Gaigai Duan: Jiangsu Co-Innovation Center of Efficient Processing and Utilization of Forest Resources, International Innovation Center for Forest Chemicals and Materials, College of Materials Science and Engineering, Nanjing Forestry University, Nanjing 210037, China

However, the development of highly selective uranium adsorbent from seawater is still a significant challenge, because the concentration of uranium is only about 3.3 ppb, and a large number of coexisting metal ions may interfere with uranium adsorption in seawater (25). In the current uranium adsorbents, such as inorganic materials (26,27), synthetic polymers (28–30), nanoporous materials (31,32), and biological materials (33,34), metal–organic framework (MOF)-based adsorbing materials as one of the nanoporous materials have been widely used, because of their unique structure and specific functional sites, which can achieve high selective adsorption of uranium in marine environment (35–39). For example, Carboni et al. first reported phosphate functionalized UiO-68 MOFs could capture uranium with a maximum uranium adsorption capacity of 217 $mg \cdot g^{-1}$ from simulated seawater (36). Based on the affinity of amidoxime group to uranyl ions (22,40), Chen et al. first presented an amidoxime functionalized UiO-66 in uranium extraction from seawater, which can eliminate 94.8% of uranyl ion within 120 min (41). However, the above MOF adsorbents are commonly used as solid powder state, it seriously limits its recycling and reusing in uranium extraction. MOF composite materials have been widely used in energy and separation fields (42) and recently also reported for uranium extraction (43). Therefore, it is necessary to combine MOFs with other matrix to prepare composite materials, which can solve the difficult separation of MOFs powder in practical use. Graphene oxide (GO) is a two-dimensional nanomaterial with wide application prospect in many fields such as photoelectric and adsorption separation (44–46). A large number of hydroxyl, carboxyl, and other oxygen-containing functional groups are distributed on the GO-based surface (47–49), which has limited adsorption performance for heavy metal ions but has weak selective U-adsorption (50). As an additive, the hydrophilic functional group of the GO can increase the hydrophilic properties of the composite, and its stable two-dimensional lamellar structure can make the composite have a high osmotic flux.

Herein, we have developed a new MOF–poly(amidoxime) (PAO) composite membrane with permeable macroporous structure, good mechanical property, and highly efficient for uranium extraction from seawater. PAO is a kind of high-performance uranium adsorbent derived from polyacrylonitrile (PAN) oxime reaction (22,51), so PAO-modified MOF can achieve better uranium extraction effect. The chemical structure of UiO-66@PAO and the selective extraction mechanism of uranium by the MOF@PAO porous membrane are shown in Scheme 1.

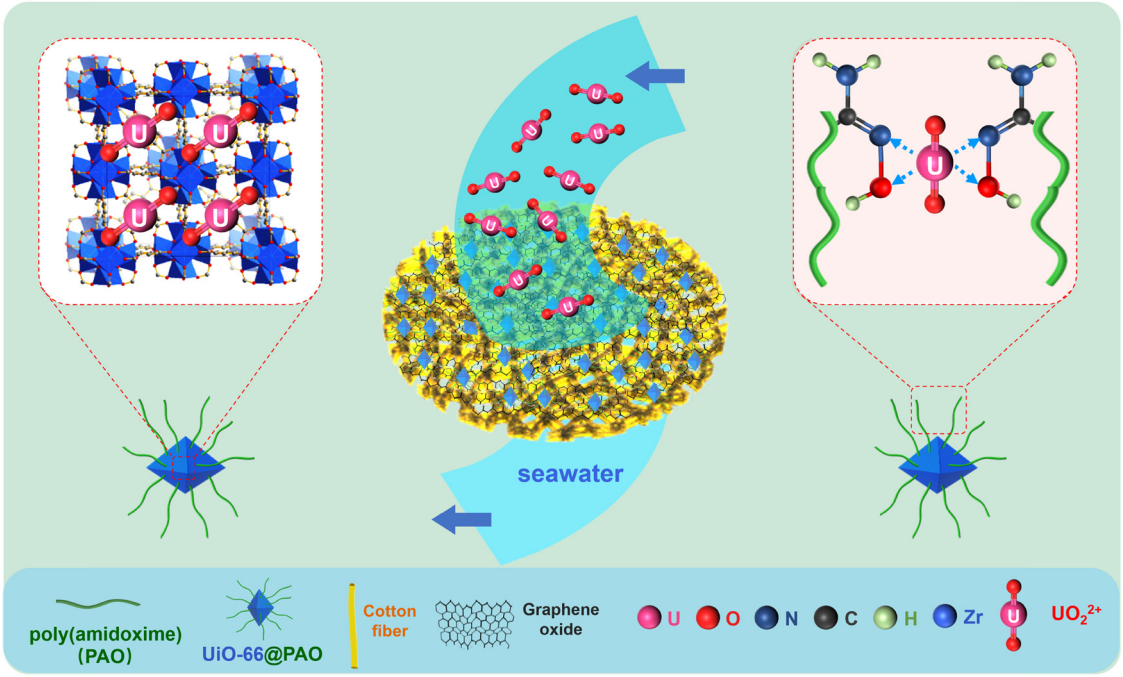

Scheme 1: The chemical structure of UiO-66@PAO and the schematic process of selective uranium adsorption by the MOF@PAO macroporous membrane.

A small amount of GOs and cotton fibers were added into the solution of UiO-66@PAO nanoparticles prepared by the amidoxime reaction of UiO-66@PAN, and the UiO-66@PAO macroporous membrane with good dispersibility, toughness, and hydrophilicity can be obtained by filtration device. Different from the original UiO-66 powder, this UiO-66@PAO macroporous composite membrane not only shows good stability and reusability in seawater but also has rapid and high-efficient uranium extraction properties. After 50 cycles of filtering 5 L natural seawater, this membrane (100 mg) can adsorb approximately 80.6% of uranium, which will be a prospective candidate for the uranium recovery from seawater.

2 Materials and methods

2.1 Materials

Terephthalic acid (TPA, 99%), PAN (average M_w = 150,000), hydroxylammonium chloride ($NH_2OH{\cdot}HCl$, 98.5%), *N*,*N*-dimethylformamide (DMF, 99.5%), and methanol (99.5%) were purchased from Macklin. Zirconium (IV) chloride ($ZrCl_4$, 99.9%) was purchased from Aladdin. Acetic acid (CH_3COOH, 99.5%) and sodium carbonate anhydrous (Na_2CO_3) were purchased from Xilong Scientific Co., Ltd. GO solution (5 mg·mL^{-1}) was purchased from XFNano Co., Ltd. Cotton fibers were purchased from Yinying Chemical Fiber Co., Ltd. [$UO_2(NO_3)_2{\cdot}6H_2O$] (99.0%), $VOSO_4{\cdot}xH_2O$ (98.5%), $NiCl_2{\cdot}6H_2O$ (98.5%), $Mn(NO_3)_2{\cdot}4H_2O$ (98.0%), $FeCl_3{\cdot}6H_2O$ (99.5%), $CuSO_4{\cdot}5H_2O$ (99.5%), $CoCl_2{\cdot}6H_2O$, (99.0%), and $Ba(NO_3)_2$ (99.5%) were purchased from Chushengwei Chemical Co., Ltd. All of the chemical reagents were analytical grade and used in this study without further purification. The seawater was fetched from the sea near the Hainan Island (Wanning City, China) and was filtered through a 0.45 μm filter membrane.

2.2 Characterization

Fourier-transform infrared spectroscopy (FT-IR) was performed with a Nicolet 7199 spectrometer. Thermo-gravimetric analysis (TGA) measurements were carried out at a heating rate of 10°C·min^{-1} through TGA Q50 TA instrument under N_2 atmosphere. Nitrogen adsorption isotherms were taken at 77 K using an ASAP2460 volumetric adsorption analyzer; the sample was dried and degassed in vacuum at 200°C for 12 h before measurements. Specific surface area of UiO-66 and UiO-66@PAO was detected through the Brunauer–Emmett–Teller method. Microstructures and morphologies of UiO-66, UiO-66@PAO, and the porous membrane were researched via a transmission electron microscopy (TEM; JEOL, JEM 2100) and a scanning electron microscopy (FE-SEM, Hitachi, S-4800). X-ray diffraction (XRD) tests were performed by using an X-ray diffractometer (AXIS SUPRA, Kratos) with a Cu-Kα radiation source (λ = 1.5406 Å). X-ray photoelectron spectroscopy (XPS) measurements were obtained with a Thermo Scientific Escalab 250Xi spectrometer. pH values of the U-added simulated seawater were detected via a pH meter (F2, Mettler Toledo). Ultraviolet-visible (UV-Vis) absorption spectra were performed with a spectrophotometer (UV1800PC, AuCy Instrument, China). The adsorption capacity of the membrane in low-concentration simulated seawater was measured by ICP-OES (iCAP 7600, Thermo Scientific, USA). The adsorption capacity of the membrane in natural seawater was measured by inductively coupled plasma mass spectrometer (ICP-MS, Agilent ICPMS7800, USA). The hydrophilic property of the UiO-66@PAO membrane was measured via a contact angle measuring instrument (Theta Flow, Biolin, Finland). The mechanical properties of the membrane were detected through a universal material testing machine (GP-6113A, Germany).

2.3 Preparation of the UiO-66

The UiO-66 was synthesized according to the previous reports (52). $ZrCl_4$ (0.5825 g), TPA (0.4152 g), and CH_3COOH (4.5 g) were dissolved within 20 mL DMF by ultrasonic, and then the mixture was poured into a 100 mL Teflon-lined autoclave and reacted at 120°C for 24 h. After cooling, the product of UiO-66 was collected through centrifugation (7,000 rpm, 20 min), and washed with DMF three times, and finally dried under vacuum (12 h, 60°C).

2.4 Preparation of the UiO-66@PAO

$ZrCl_4$ (0.5825 g), TPA (0.4152 g), CH_3COOH (4.5 g), and PAN (0.4857 g) were dissolved within 20 mL DMF by ultrasound. Then, the mixture was poured into the 100 mL Teflon-lined autoclave and reacted at 120°C for 24 h. After cooling at room temperature, the product of UiO-66@PAN was collected via centrifugation (7,000 rpm, 20 min), and washed with DMF three times, and finally dried

under vacuum (12 h, 60°C). For preparing UiO-66@PAO, UiO-66@PAN (1 g) was added into DMF solution (10 mL) containing $NH_2OH{\cdot}HCl$ (0.65 g) and Na_2CO_3, with the pH reached 6.5–7. Then, the mixture was stirred at 65°C for 12 h. After reaction, the obtained UiO-66@PAO materials were repeated centrifugation and precipitation from methanol for three times.

2.5 Preparation of the UiO-66@PAO porous membrane

The UiO-66@PAO (90 mg) was dispersed into 5 mL DMF solution by ultrasound for 20 min. After 1 mL GO solution (5 mg·mL^{-1}) was mixed and stirred for 30 min, 5 mg of cotton fibers were added and stirred vigorously for 60 min. The length and diameters of cotton fibers were 450 ± 250 and 13 ± 2 μm, respectively (Figure S1 in Supplementary material). The UiO-66@PAO porous membrane was prepared by high pressure suction filter. A typical experiment was conducted as follows: 6 mL mixture was filtered through a 0.45 μm filter paper to form a tough UiO-66@PAO porous membrane. This composite membrane was dried and kept in the seal at room temperature.

2.6 Test method for pure water flux

Membrane flux experiments were carried out with a filtration apparatus. UiO-66@PAO membrane samples were covered on the filter screen. Vacuum pump is used to create pressure difference. The pure water flux of UiO-66@PAO membrane was calculated based on the passed water volume through the membrane per second per square area using Eq. 1 (53):

$$J = \frac{V}{A \cdot t} \tag{1}$$

where J is the water flux (L·m^{-2}·h^{-1}), V is the passed water volume, A is the effective area of the UiO-66@PAO membrane (m^2), and t is time (s).

2.7 Test of the uranium adsorption performance

The UV-Vis absorption spectrum of arsenazo(III) was used to determine the concentrations of U-added simulated seawater. The obtained uranium concentration absorbance curve in U-added simulated seawater is shown in Figure S2.

The uranium adsorbing capacity was calculated using Eq. 2:

$$Q_{\text{Membrane}} = W_{\text{U}}/W_{\text{Membrane}} \tag{2}$$

where Q_{Membrane} is the uranium adsorbing amounts of the UiO-66@PAO porous membrane (mg·g^{-1}), W_{U} and W_{Membtane} are the mass of the uranium (mg) and the mass of UiO-66@PAO porous membrane (g), respectively.

The uranium adsorption performance can be examined by the pseudo-first-order and pseudo-second-order adsorption kinetic in Eqs. 3 and 4:

$$\ln(q_e - q_t) = \ln q_e - k_1 t \tag{3}$$

$$\frac{t}{q_t} = \frac{1}{K_2 q_e^2} + \frac{t}{q_e} \tag{4}$$

where t is U-adsorbing time (min); k_1 (min^{-1}) and k_2 (g·mg^{-1}·min^{-1}) are the adsorption rate constants for pseudo-first-order and pseudo-second-order kinetic models, respectively; q_t is the uranium absorption amounts at exposure time (mg·g^{-1}) of UiO-66@PAO membrane after a specific time; q_e is the uranium absorption amounts (mg·g^{-1}) of UiO-66@PAO membrane at the equilibrium state.

2.8 Method of the U-adsorption from low-concentration U-added pure water and natural seawater

A continuous filtration separation device with a peristaltic pump was used to extract uranium from pure water at low concentrations of uranium. The UiO-66@PAO (100 mg) membrane was placed between two thin sponges, and the flow rate of 1 L low-concentration uranium pure water was controlled at 50 mL·min^{-1} using a peristaltic pump. Then, 2 mL of liquid samples were extracted from the U-added water every 20 min and analyzed by ICP-MS. In addition, 5 L natural seawater was used for testing, and the liquid samples were analyzed by ICP-MS.

2.9 Adsorption–desorption cycle test

The uranium-containing samples adsorbed for 10 cycles in 60 ppb U-added water were placed into 0.1 M HCl

solution (50 mL) at 50°C for 0.5 h. Then, 2 mL liquid samples were collected and analyzed by ICP-OES. The membrane was washed with deionized water until the wash solution pH = 7, and the washed membrane was used for the next uranium adsorption.

3 Results and discussion

3.1 Fabrication and characterization of the MOFs

To introduce PAO into MOFs, we first prepare functional UiO-66@PAN nanoparticles via hydrothemal method. PAN can be changed into PAO by the amidoximation reaction. Under alkaline conditions, PAN will undergo amidoximation reaction with hydroxylamine hydrochloride to convert into PAO. That is to say UiO-66@PAN could further transfer into UiO-66@PAO nanoparticles (Figure 1a). The FT-IR spectroscopy was used to characterize UiO-66@PAN and UiO-66@PAO (Figure 1b). The UiO-66@PAN has an obvious absorption peak of nitrile group (−C≡N) at 2,246 cm^{-1}. After amidoximation reaction, the −C≡N absorption peak vanished entirely and the characteristic peaks of oxime group with C═N (1,638 cm^{-1}), C–N (1,381 cm^{-1}), and N–O (933 cm^{-1}) appeared, which proved the successful transformation. To prove the existence of the nanoporous structure of UiO-66 and UiO-66@PAO (Figure 1c), N_2 adsorption was used to estimate the permanent porosities of MOFs (52). Both UiO-66 and UiO-66@PAO were Type-I curves, which verified UiO-66@PAO owning good nanoporous structure (Figure 1d). Compared with UiO-66, the modified UiO-66@PAO has ultrahigh specific surface area just slightly reduced from 1,170 to 1,079 $m^2 \cdot g^{-1}$, which can provide the high-speed uranium adsorbing process. As illustrated in Figure 1e, the positions of specific XRD peaks of UiO-66 and UiO-66@PAO almost remain unchanged, which can confirm that the UiO-66@PAO keep the original crystal structure well after being modified by the PAO. Furthermore, the SEM and TEM images of them were also characterized. The results indicated that UiO-66@PAO had well-constructed octahedron morphologies, which had no obvious morphology change with UiO-66 (Figure 1e and f). Moreover, the energy dispersive spectrometer (EDS) mappings of UiO-66@PAO further verify the chemical composition including Zr, C, O, and N elements (Figure S3). The TGA results showed that the UiO-66@PAO has a clear weight loss of PAO (Figure S4).

3.2 Fabrication and characterization of the UiO-66@PAO membrane

It is important to combine MOFs with matrix to prepare a MOF-based composite membrane. The key factor is how to disperse UiO-66@PAO in the hybrid membrane. The fabrication of the UiO-66@PAO porous membrane by a fast and simple method via a sand core funnel filter device is exhibited in Figure 2a, the membrane can easily be rolled, which shows a good flexibility. The good flexibility was largely determined by the addition of cotton fibers, and the effect of different proportion of it on the tensile strength of the membrane was studied. When the addition amount of cotton fibers was less than 5%, the strength of the membrane increased gradually with its addition, and reached the tensile strength of 0.938 ± 0.104 MPa when the addition amount was 5%. However, when the content of cotton fibers continued to increase, the strength of the membrane will not change significantly, so 5% was an appropriate proportion (Figure S5). To prepare the MOF-based membrane, we systematically studied the dispersibility of the MOFs in fluids and successfully solved the easily precipitation problem. As shown in Figure 2b, the direct dispersion of UiO-66@PAO in DMF solution will quickly settle, which will seriously affect the formation of the membrane with high strength and uniform porous structure. To solve this problem, GO was used to disperse UiO-66@PAO. When the mass ratio of GO to MOF was 1:18, the UiO-66@PAO can be evenly dispersed in DMF solution, which could leave alone for 4 weeks without precipitation. This may attribute to the coordination between metal sites of MOFs and oxygen-containing functional groups on GO (54,55). The change of the contact angles between the UiO-66@PAO nanoparticles and the UiO-66@PAO macroporous membrane was measured by a contact angle meter. The results indicated that the hydrophilicity of UiO-66@PAO composites membrane have been improved greatly, compared with the original UiO-66@PAO (Figure 2c). The reasons may be the compositions of super-hydrophilic GO/cotton fibers and the porous structure in the membrane. Using a small amount of GOs and cotton fibers, macroporous membrane structure was formed.

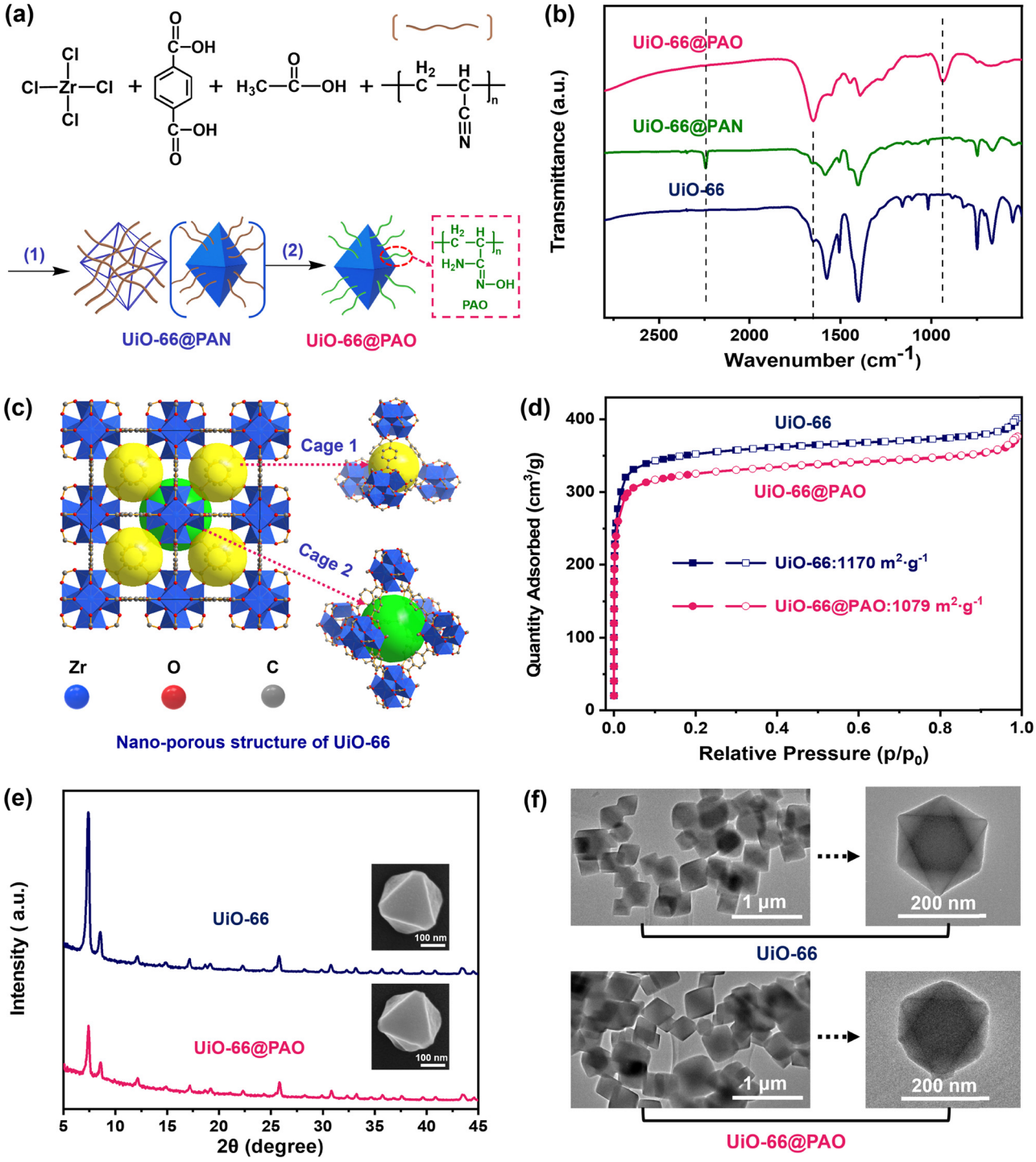

Figure 1: (a) Synthesis of UiO-66@PAO and the illustration of change on MOF surface. (b) The FT-IR spectra of UiO-66, UiO-66@PAN, and UiO-66@PAO. (c) The 3D nanostructure of the UiO-66. (d) The N_2 adsorption–desorption isotherms. (e) The XRD, SEM images. (f) The TEM images of different MOFs, including UiO-66, UiO-66@PAN, and UiO-66@PAO.

As shown in Figure S6, the pore size of MOF@PAO composite membrane was about 500 nm to 2 μm and changed little before and after use, which gave the membrane excellent pure water flux. As illustrated in Figure 2d, the flux value can reach 5,000 $L \cdot m^{-2} \cdot h^{-1}$ at 95 kPa water pressure and the membrane does not break.

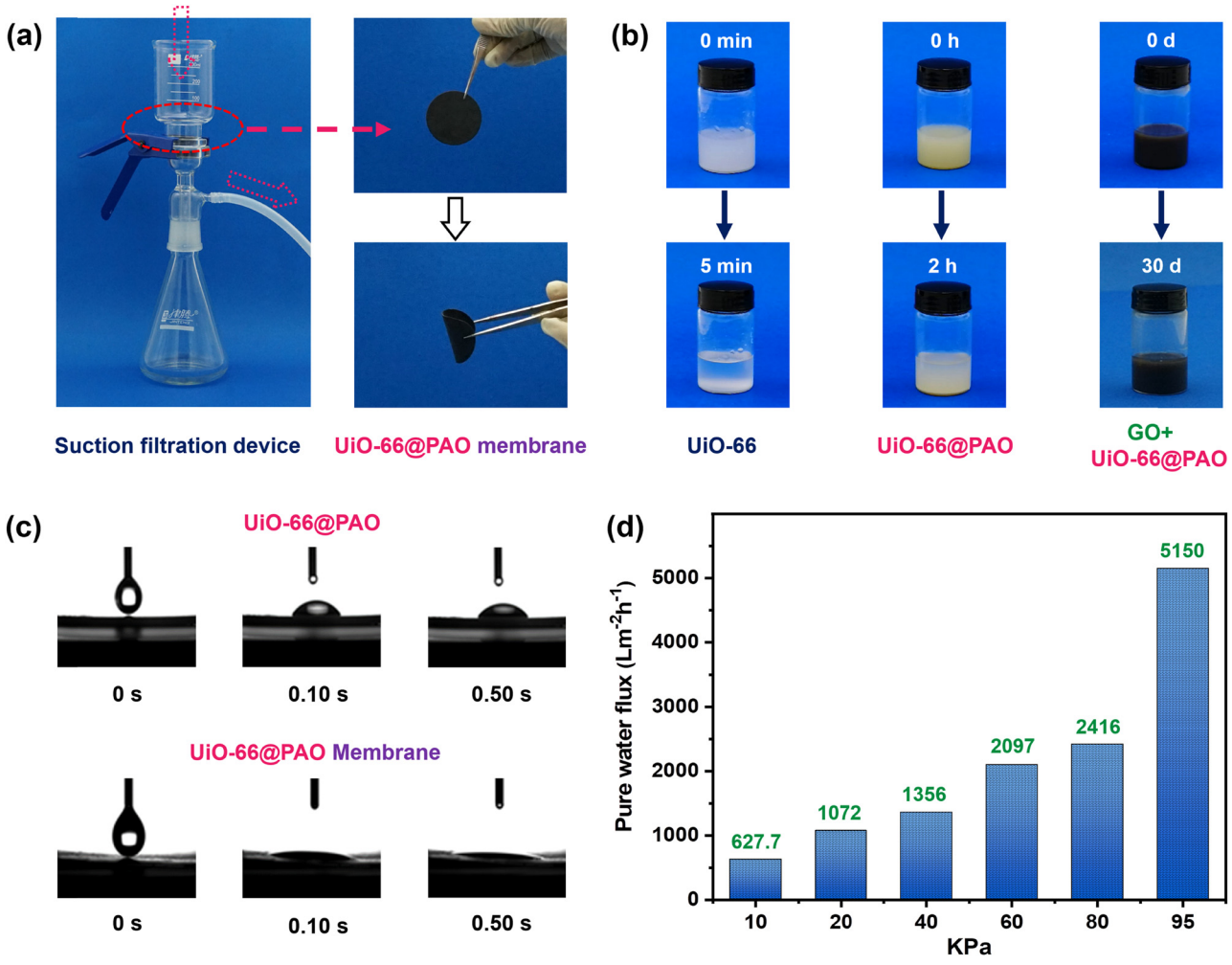

Figure 2: (a) The preparation of the UiO-66@PAO porous membrane. (b) The dispersion of UiO-66, UiO-66@PAO, and UiO-66@PAO containing GO in DMF solution, respectively. (c) The contact angles of UiO-66@PAO powder and UiO-66@PAO membrane. (d) The pure water flux of UiO-66@PAO porous membrane at different pressures.

3.3 Uranium adsorption performance of UiO-66@PAO membrane from U-added simulated seawater

Then, the uranium adsorption property of the UiO-66@PAO membrane was investigated in U-added simulated seawater. After the immersion of the membrane in 32 ppm U-added simulated seawater, the UiO-66@PAO membrane transformed to UiO-66@PAO-U membrane, both of them were characterized by XPS (Figure 3a). Compared with UiO-66@PAO membrane, the UiO-66@PAO-U membrane exhibited strong $U4f_{5/2}$ and $U4f_{7/2}$ bimodality, which located at the 392.65 and 381.60 bond energies, indicating that the UiO-66@PAO membrane exhibited uranium adsorbing property. Moreover, the uranium adsorbing performance of the UiO-66@PAO macroporous membrane was demonstrated via EDS mapping. In contrast to the original membrane, after absorbing uranium in 8 ppm U-added simulated seawater for 8 h, the U-uptake membrane had a strong and uniform uranium distribution (Figure 3b). Moreover, the U-uptake membrane in Figure S6 appeared as two specific peaks of the uranium (3.18 and 3.35 keV). pH is a significant factor affecting the uranium adsorption capacity of this UiO-66@PAO membrane. According to Figure 3c, the uranium absorption performance was the best at pH = 6. It should be noted that even in alkaline seawater (pH = 8.0), the amount of uranium extracted can reach 326 ± 17.4 $mg \cdot g^{-1}$, which confirms that the UiO-66@PAO membrane still has good adsorption properties in seawater. To explore

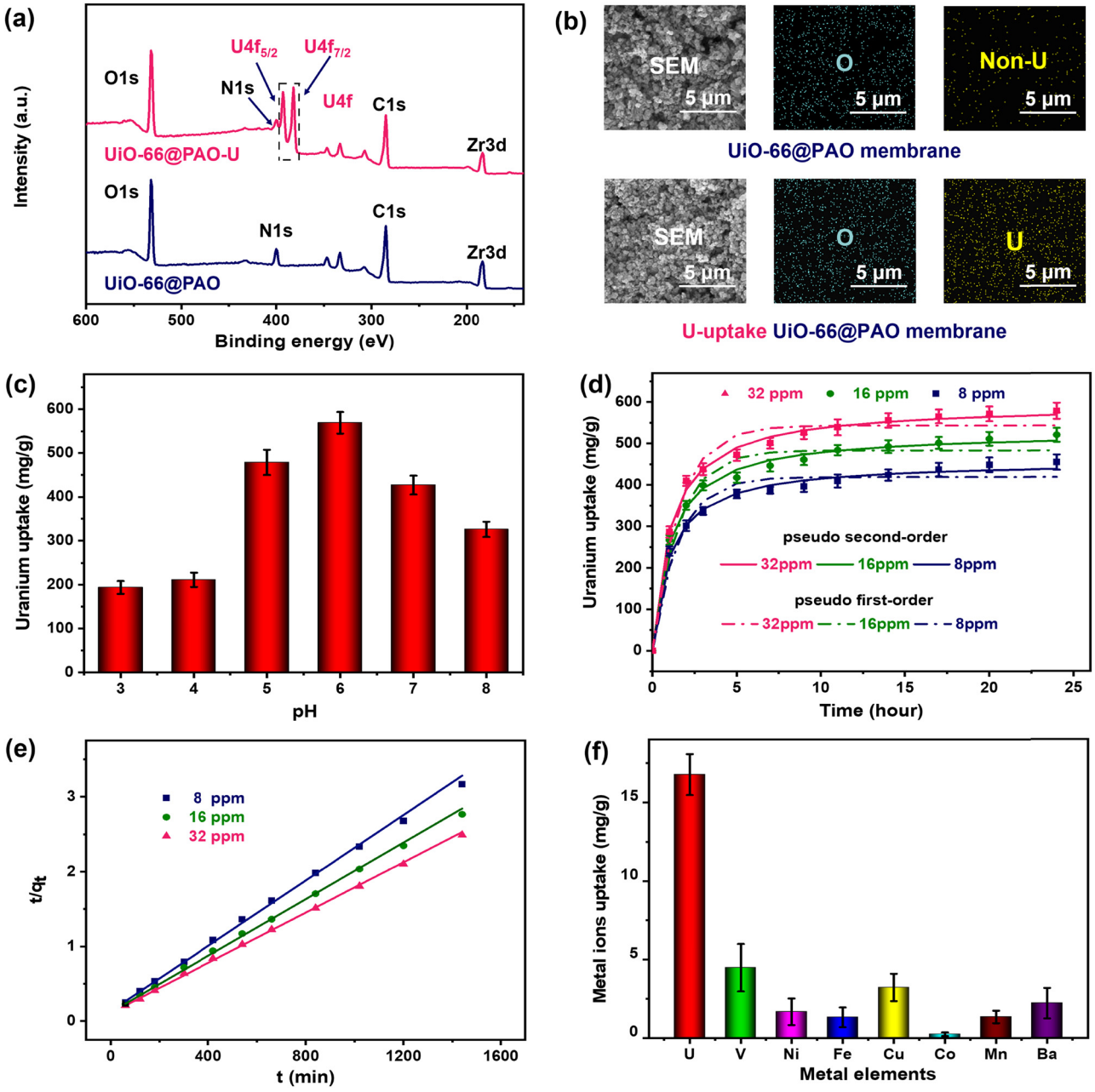

Figure 3: (a) The XPS spectra. (b) The SEM images and EDS mappings of UiO-66@PAO membrane before and after U-uptake. (c) The U-adsorption performance of UiO-66@PAO membrane in 32 ppm U-added simulated seawater under different pH values. (d and e) U-adsorption kinetics of UiO-66@PAO membrane and the pseudo-second-order models in 8, 16, 32 ppm U-added simulated seawater, respectively. (f) Adsorbing specificity of the UiO-66@PAO membrane for different metal ions in simulated seawater.

the best effect of uranium extraction, uranium absorption experiments were performed in U-added simulated seawater at pH = 6 with different uranium concentrations (8, 16, 32 ppm). The UiO-66@PAO membrane exhibited ultra-fast and high uranium extraction performance illustrated by adsorption kinetics curves (Figure 3d). After 1 h, UiO-66@PAO membrane could extract uranium up to 240 ± 11.5, 267 ± 11.2, and 286 ± 12.4 mg·g^{-1} at U-added simulated seawater with concentrations ranging from 8 to 32 ppm. After 24 h, they were saturated to 455 ± 18.4, 521 ± 16.8, and 579 ± 19.4 mg·g^{-1}, respectively. Furthermore, the high degree of the fit between the U-adsorbing curves and the pseudo-second-order kinetics as shown in Figure 3e confirmed the U-adsorbing behavior of

the UiO-66@PAO membrane belong to a kind of chemical adsorbing behavior. The excellent linearity of the function about (t/qt)-t and the correlation coefficients of Eq. 4 with more than 0.990 in Table S1 (in Supplementary material). A comparative experiment was designed to investigate the effect of GO nanosheets in UiO-66@PAO membrane on uranium extraction. In the comparison sample, the content of MOF was replaced by cotton fiber, and the proportion of GO is the same as the original UiO-66@PAO membrane. The uranium adsorption performance of UiO-66@PAO membrane and GO@Cotton fiber membrane was tested in 32 ppm U-added simulated seawater (pH = 6). As we can see from Figure S7, the uranium adsorption capacity of GO@Cotton fiber is much lower than UiO-66@PAO membrane, this is due to the fact that the GO added is very little, the effect of GO on uranium extraction can be ignored. In this study, above results showed that the UiO-66@PAO membrane had a very high uranium extraction performance among most of existing MOF-based uranium adsorbing materials (Table S2). There are numerous coexisting metal ions in seawater. Therefore, it is necessary to test ion selectivity of UiO-66@PAO membrane in simulated seawater with 100 times higher ion concentration than natural seawater (Table S3). As shown in Figure 3f, the uranium adsorption capacity of UiO-66@PAO membrane is higher than other metal elements including vanadium in seawater, indicating that it had a good application for high selective seawater uranium extraction. For traditional amidoxime functionalized materials, the competitive adsorption of vanadium and uranium is almost the same (28). Interestingly, the UiO-66@PAO membrane has a higher uranium selective adsorption than vanadium, which may be because of the unique PAO-modified MOF structure.

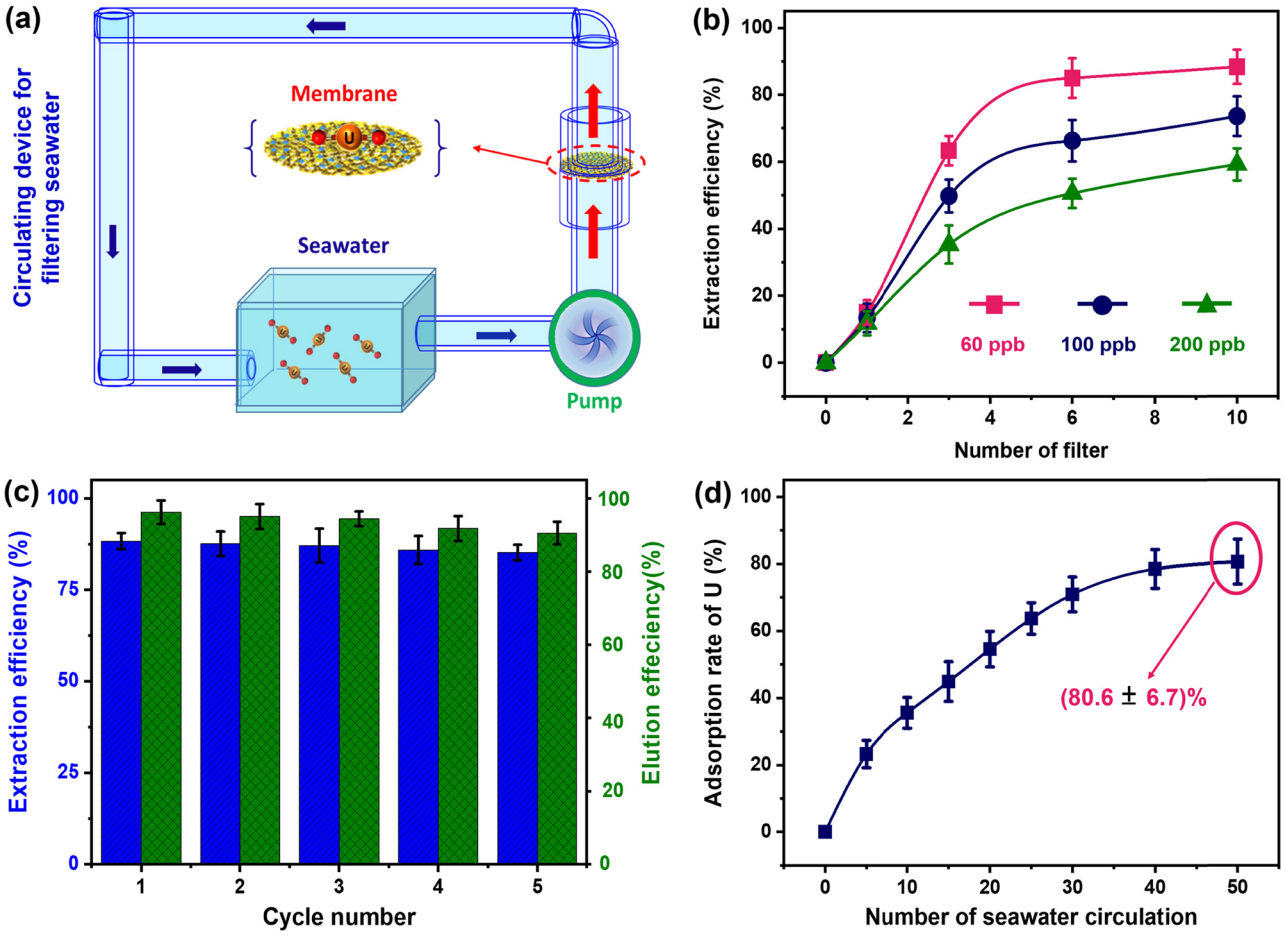

Figure 4: (a) The schematic of seawater uranium extraction device. (b) The U-extraction rate of UiO-66@PAO membrane with 60, 100, and 200 ppb uranium-spiked ultrapure water. (c) U-adsorbing performance and U-recovery rates in five adsorbing/desorbing cycles. (d) U-extraction rate of UiO-66@PAO membrane (100 mg) in 5 L of nature seawater for 50 cycles.

3.4 Uranium adsorption from low-concentration U-added pure water and natural seawater

To evaluate the adsorption property of the UiO-66@PAO membrane exposed in real applications (e.g., ultralow concentration of uranium-added solutions, the natural seawater), a continuous filtration separation device with a peristaltic pump has been designed (Figure 4a). After 10 cycles of filtration with the UiO-66@PAO macroporous membrane (100 mg), the results indicated that it could extract up to 88.33%, 70%, and 50% of uranium from 60, 100, and 200 ppb concentration U-added pure water, respectively (Figure 4b). To be noted, for 60 ppb U-added solution, the uranium had been largely removed by the membrane in the six cycles, which demonstrated the highly efficient and rapid uranium adsorbing performance of this membrane. The reusability of the adsorbed materials is a critical factor in practical use. After five cycles of adsorption/desorption process, the results, as shown in Figure 4c, showed that the uranium extraction efficiency of UiO-66@PAO macroporous membrane still could reach 80% in 60 ppb U-spiked water, and the eluent rate could reach 88%. At last, untreated real seawater was added into the filtration separation device to estimate the performance of UiO-66@PAO membranes for uranium extraction in real marine environments. As illustrated in Figure 4d, the UiO-66@PAO porous membrane extracted approximately 80.6% of uranium from 5 L seawater after 50 cycles of filtration. These results proved that the UiO-66@PAO porous membrane was an outstanding adsorbent with high reusability.

4 Conclusions

In conclusion, a simple and rapid approach for manufacturing UiO-66@PAO composite porous membrane via simple suction filtration has been developed, which can achieve highly efficient and selective uranium adsorption performance. Compared with nonmodified UiO-66, this UiO-66@PAO not only can be dispersed uniformly in the membrane owing to the well stabilization in the GO solution but also can largely enhance the uranium adsorbing capacity due to the modified PAO. Furthermore, different from powder state, this UiO-66@PAO macroporous membrane can provide both convenient and highly efficient uranium adsorption from seawater, because of the flux macroporous structure without sacrificing high specific surface area of the MOF in the membrane. As a result, the uranium adsorption capacity of this membrane can reach 579 $mg \cdot g^{-1}$ in 32 ppm U-spiked simulated seawater for only 24 h. Furthermore, in a 60 ppb of ultra-low U-spiked pure water, this membrane can provide a high uranium extraction rate reaching 88.4%. Most importantly, this UiO-66@PAO membrane (100 mg) can remove 80.6% uranyl ions from 5 L seawater after 50 filtering cycles. This study provides a universal method to design and fabricate a new MOF-based adsorbent for high efficiency uranium extraction from seawater.

Funding information: This work was supported by the National Natural Science Foundations of China (No. 21965010, 22065012, 51775152, 61761016, U1967213, 41966009), the Hainan Science and Technology Major Project (ZDKJ2020011 and ZDKJ2019013), the Hainan Provincial Natural Science Foundation of China (2019CXTD401), the Taizhou-Zhejiang University Science and Technology Program (2018NMS01), the Taizhou Innovation Centre Science Park Special Fund (QTKJ201903001), the National Key R&D program of China (2018YFE0103500), the Finance Science and Technology Project of Hainan Province (No. ZDYF2020205), and the Research Foundations of Hainan University [KYQD(ZR)1811, KYQD(ZR)1814, KYQD(ZR)1815].

Author contributions: Jiawen Wang: writing – original draft, writing – review and editing, formal analysis, investigation; Ye Sun: writing – review and editing and resources; Xuemei Zhao: writing – review and editing, methodology; Lin Chen: writing – review and editing; Shuyi Peng: writing – review and editing and investigation; Chunxin Ma: writing – review and editing, investigation, resources; Gaigai Duan: writing – review and editing; Zhenzhong Liu: writing – review and editing, investigation, methodology; Hui Wang: resources; Yihui Yuan: project administration; Ning Wang: conceptualization, writing – review and editing.

Conflict of interest: Author states no conflict of interest.

Data availability statement: All data generated or analyzed during this study are included in this published article and its supplementary information files.

References

(1) Schiermeier Q, Tollefson J, Scully T, Witze A, Morton O. Energy alternatives: electricity without carbon. Nature. 2008;454(7206):816–23. doi: 10.1038/454816a.
(2) Sholl DS, Lively RP. Seven chemical separations to change the world. Nature. 2016;532(7600):435–7. doi: 10.1038/532435a.

(3) Sun Y, Ding C, Cheng W, Wang X. Simultaneous adsorption and reduction of U(VI) on reduced graphene oxide-supported nanoscale zerovalent iron. J Hazard Mater. 2014;280:399–408. doi: 10.1016/j.jhazmat.2014.08.023.
(4) Liu C, Hsu P-C, Xie J, Zhao J, Wu T, Wang H, et al. A half-wave rectified alternating current electrochemical method for uranium extraction from seawater. Nat Energy. 2017;2(4):17007. doi: 10.1038/nenergy.2017.7.
(5) Feng M-L, Sarma D, Qi X-H, Du K-Z, Huang X-Y, Kanatzidis MG. Efficient removal and recovery of uranium by a layered organic-inorganic hybrid thiostannate. J Am Chem Soc. 2016;138(38):12578–85. doi: 10.1021/jacs.6b07351.
(6) Liu W, Zhao X, Wang T, Zhao D, Ni J. Adsorption of U(VI) by multilayer titanate nanotubes: effects of inorganic cations, carbonate and natural organic matter. Chem Eng J. 2016;286:427–35. doi: 10.1016/j.cej.2015.10.094.
(7) Manos MJ, Kanatzidis MG. Layered metal sulfides capture uranium from seawater. J Am Chem Soc. 2012;134(39):16441–6. doi: 10.1021/ja308028n.
(8) Veliscek-Carolan J. Separation of actinides from spent nuclear fuel: a review. J Hazard Mater. 2016;318:266–81. doi: 10.1016/j.jhazmat.2016.07.027.
(9) Kumar JR, Kim J-S, Lee J-Y, Yoon H-S. A brief review on solvent extraction of uranium from acidic solutions. Sep Purif Rev. 2011;40(2):77–125. doi: 10.1080/15422119.2010.549760.
(10) St , John AM, Cattrall RW, Kolev SD. Extraction of uranium(VI) from sulfate solutions using a polymer inclusion membrane containing di-(2-ethylhexyl) phosphoric acid. J Membr Sci. 2010;364(1-2):354–61. doi: 10.1016/j.memsci.2010.08.039.
(11) Yuan Y, Yu Q, Wen J, Li C, Guo Z, Wang X, et al. Ultrafast and highly selective uranium extraction from seawater by hydrogel-like spidroin-based protein fiber. Angew Chem Int Ed. 2019;58(34):11785–90. doi: 10.1002/anie.201906191.
(12) Yuan Y, Feng S, Feng L, Yu Q, Liu T, Wang N. A bio-inspired nano-pocket spatial structure for targeting uranyl capture. Angew Chem Int Ed. 2020;59(11):4262–8. doi: 10.1002/anie.201916450.
(13) Lin K, Sun W, Feng L, Wang H, Feng T, Zhang J, et al. Kelp inspired bio-hydrogel with high antibiofouling activity and super-toughness for ultrafast uranium extraction from seawater. Chem Eng J. 2022;430:133121. doi: 10.1016/j.cej.2021.133121.
(14) Sun Q, Aguila B, Earl LD, Abney CW, Wojtas L, Thallapally PK, et al. Covalent organic frameworks as a decorating platform for utilization and affinity enhancement of chelating sites for radionuclide sequestration. Adv Mater. 2018;30(20):1705479. doi: 10.1002/adma.201705479.
(15) Chen M, Liu T, Zhang X, Zhang R, Tang S, Yuan Y, et al. Photoinduced enhancement of uranium extraction from seawater by MOF/black phosphorus quantum dots heterojunction anchored on cellulose nanofiber aerogel. Adv Funct Mater. 2021;31(22):2100106. doi: 10.1002/adfm.202100106.
(16) Shi S, Li B, Qian Y, Mei P, Wang N. A simple and universal strategy to construct robust and anti-biofouling amidoxime aerogels for enhanced uranium extraction from seawater. Chem Eng J. 2020;397:125337. doi: 10.1016/j.cej.2020.125337.
(17) Yan B, Ma C, Gao J, Yuan Y, Wang N. An ion-crosslinked supramolecular hydrogel for ultrahigh and fast uranium recovery from seawater. Adv Mater. 2020;32(10):e1906615. doi: 10.1002/adma.201906615.
(18) Liu R, Wen S, Sun Y, Yan B, Wang J, Chen L, et al. A nanoclay enhanced amidoxime-functionalized double-network hydrogel for fast and massive uranium recovery from seawater. Chem Eng J. 2021;422:130060. doi: 10.1016/j.cej.2021.130060.
(19) Ma C, Gao J, Wang D, Yuan Y, Wen J, Yan B, et al. Sunlight polymerization of poly(amidoxime) hydrogel membrane for enhanced uranium extraction from seawater. Adv Sci. 2019;6(13):1900085. doi: 10.1002/advs.201900085.
(20) Saad EM, Elshaarawy RF, Mahmoud SA, El-Moselhy KM. New ulva lactuca algae based chitosan bio-composites for bioremediation of Cd(II) ions. J Bioresour Bioprod. 2021;6(3):223–42. doi: 10.1016/j.jobab.2021.04.002.
(21) Wei D, Wei Z, Kaneshiro H, Wang Y, Lin H, Pen S. Preparation of bamboo charcoal pottery and its gas adsorption and humidity regulation performance. J For Eng. 2020;5(1):109–13. doi: 10.13360/j.issn.2096-1359.201905025.
(22) Abney CW, Mayes RT, Saito T, Dai S. Materials for the recovery of uranium from seawater. Chem Rev. 2017;117(23):13935–4013. doi: 10.1021/acs.chemrev.7b00355.
(23) Jjagwe J, Olupot PW, Menya E, Kalibbala HM. Synthesis and application of granular activated carbon from biomass waste materials for water treatment: a review. J Bioresour Bioprod. 2021;6(4):292–322. doi: 10.1016/j.jobab.2021.03.003.
(24) Wang Z, Hu C, Tu D, Zhang W, Guan L. Preparation and adsorption property of activated carbon made from Camellia olerea shells. J For Eng. 2020;5(5):96–102. doi: 10.13360/j.issn.2096-1359.202001032.
(25) Barbano PG, Rigali L. Spectrophotometric determination of uranium in sea water after extraction with aliquat-336. Anal Chim Acta. 1978;96(1):199–201. doi: 10.1016/S0003-2670(01)93415-4.
(26) Chen HJ, Chen Z, Zhao GX, Zhang ZB, Xu C, Liu YH, et al. Enhanced enhanced adsorption of U(VI) and Am-241(III) from wastewater using Ca/Al layered double hydroxide@carbon nanotube composites. J Hazard Mater. 2018;347:67–77. doi: 10.1016/j.jhazmat.2017.12.062.
(27) Chen H, Chen Z, Zhao G, Zhang Z, Xu C, Liu Y, et al. Enhanced enhanced adsorption of U(VI) and Am-241(III) from wastewater using Ca/Al layered double hydroxide@carbon nanotube composites. J Hazard Mater. 2018;347:67–77. doi: 10.1016/j.jhazmat.2017.12.062.
(28) Xu X, Zhang HJ, Ao JX, Xu L, Liu XY, Guo XJ, et al. 3D hierarchical porous amidoxime fibers speed up uranium extraction from seawater. Energy Environ Sci. 2019;12(6):1979–88. doi: 10.1039/c9ee00626e.
(29) Ladshaw AP, Wiechert AI, Das S, Yiacoumi S, Tsouris C. Amidoxime polymers for uranium adsorption: influence of comonomers and temperature. Materials. 2017;10(11):1268. doi: 10.3390/ma10111268.
(30) Yuan D, Wang Y, Qian Y, Liu Y, Feng G, Huang B, et al. Highly selective adsorption of uranium in strong HNO3 media achieved on a phosphonic acid functionalized nanoporous polymer. J Mater Chem A. 2017;5(43):22735–42. doi: 10.1039/c7ta07320h.
(31) Xiong XH, Yu ZW, Gong L, Tao Y, Gao Z, Wang L, et al. Ammoniating covalent organic framework (COF) for high-performance and selective extraction of toxic

and radioactive uranium ions. Adv Sci. 2019;6(16):1900547. doi: 10.1002/advs.201900547.
(32) Wen R, Li Y, Zhang M, Guo X, Li X, Li X, et al. Graphene-synergized 2D covalent organic framework for adsorption: a mutual promotion strategy to achieve stabilization and functionalization simultaneously. J Hazard Mater. 2018;358:273–85. doi: 10.1016/j.jhazmat.2018.06.059.
(33) Yuan YH, Yu QH, Yang S, Wen J, Guo ZH, Wang XL, et al. Ultrafast recovery of uranium from seawater by bacillus velezensis strain UUS-1 with innate anti-biofouling activity. Adv Sci. 2019;6(18):1900961. doi: 10.1002/advs.201900961.
(34) Khani MH, Keshtkar AR, Ghannadi M, Pahlavanzadeh H. Equilibrium, kinetic and thermodynamic study of the biosorption of uranium onto Cystoseria indica algae. J Hazard Mater. 2008;150(3):612–8. doi: 10.1016/j.jhazmat.2007.05.010.
(35) Luo B-C, Yuan L-Y, Chai Z-F, Shi W-Q, Tang Q. U(VI) capture from aqueous solution by highly porous and stable MOFs: UiO-66 and its amine derivative. J Radioanal Nucl Chem. 2015;307(1):269–76. doi: 10.1007/s10967-015-4108-3.
(36) Carboni M, Abney CW, Liu SB, Lin WB. Highly porous and stable metal-organic frameworks for uranium extraction. Chem Sci. 2013;4(6):2396–402. doi: 10.1039/c3sc50230a.
(37) Li JQ, Gong LL, Feng XF, Zhang L, Wu HQ, Yan CS, et al. Direct extraction of U(VI) from alkaline solution and seawater via anion exchange by metal-organic framework. Chem Eng J. 2017;316:154–9. doi: 10.1016/j.cej.2017.01.046.
(38) Wang LL, Luo F, Dang LL, Li JQ, Wu XL, Liu SJ, et al. Ultrafast high-performance extraction of uranium from seawater without pretreatment using an acylamide- and carboxyl-functionalized metal-organic framework. J Mater Chem A. 2015;3(26):13724–30. doi: 10.1039/c5ta01972a.
(39) Zhang J, Zhang H, Liu Q, Song D, Li R, Liu P, et al. Diaminomaleonitrile functionalized double-shelled hollow MIL-101 (Cr) for selective removal of uranium from simulated seawater. Chem Eng J. 2019;368:951–8. doi: 10.1016/j.cej.2019.02.096.
(40) Abney CW, Mayes RT, Piechowicz M, Lin Z, Bryantsev VS, Veith GM, et al. XAFS investigation of polyamidoxime-bound uranyl contests the paradigm from small molecule studies. Energy Environ Sci. 2016;9(2):448–53. doi: 10.1039/C5EE02913A.
(41) Chen L, Bai Z, Zhu L, Zhang L, Cai Y, Li Y, et al. Ultrafast and efficient extraction of uranium from seawater using an amidoxime appended metal-organic framework. ACS Appl Mater Interfaces. 2017;9(38):32446–51. doi: 10.1021/acsami.7b12396.
(42) Lu C, Xiao H, Chen X. MOFs/PVA hybrid membranes with enhanced mechanical and ion-conductive properties. e-Polymers. 2021;21(1):160–5. doi: 10.1515/epoly-2021-0010.
(43) Liu T, Li Z, Zhang X, Tan H, Chen Z, Wu J, et al. Metal-organic framework-intercalated graphene oxide membranes for selective separation of uranium. Anal Chem. 2021;93(48):16175–83. doi: 10.1021/acs.analchem.1c03982.
(44) Yildiz Y, Okyay TO, Sen B, Gezer B, Kuzu S, Savk A, et al. Highly monodisperse Pt/Rh nanoparticles confined in the graphene oxide for highly efficient and reusable sorbents for methylene blue removal from aqueous solutions. Chemistryselect. 2017;2(2):697–701. doi: 10.1002/slct.201601608.
(45) Qian H, Wang J, Yan L. Synthesis of lignin-poly(N-methyl-aniline)-reduced graphene oxide hydrogel for organic dye and lead ions removal. J Bioresour Bioprod. 2020;5(3):204–10. doi: 10.1016/j.jobab.2020.07.006.
(46) Wang R, Xuelian Z, Xu T, Bian H, Dai H. Research progress on the preparation of lignin-derived carbon dots and graphene quantum dots. J For Eng. 2021;6(1):29–37. doi: 10.13360/j.issn.2096-1359.202001007.
(47) Liu S, Yang H, Sui L, Jiang S, Hou H. Self-adhesive polyimide (PI) @reduced graphene oxide (RGO)/PI@carbon nanotube (CNT) hierarchically porous electrodes: maximizing the utilization of electroactive materials for organic Li-ion batteries. Energy Technol. 2020;8(9):2000397. doi: 10.1002/ente.202000397.
(48) Cao L, Li H, Liu X, Liu S, Zhang L, Xu W, et al. Nitrogen, sulfur co-doped hierarchical carbon encapsulated in graphene with "sphere-in-layer" interconnection for high-performance supercapacitor. J Colloid Interface Sci. 2021;599:443–52. doi: 10.1016/j.jcis.2021.04.105.
(49) Zhou X, Ding C, Cheng C, Liu S, Duan G, Xu W, et al. Mechanical and thermal properties of electrospun polyimide/rGO composite nanofibers via in-situ polymerization and in-situ thermal conversion. Eur Polym J. 2020;141:110083. doi: 10.1016/j.eurpolymj.2020.110083.
(50) Sun PZ, Zhu M, Wang KL, Zhong ML, Wei JQ, Wu DH, et al. Selective ion penetration of graphene oxide membranes. Acs Nano. 2013;7(1):428–37. doi: 10.1021/nn304471w.
(51) Duan G, Liu S, Hou H. Synthesis of polyacrylonitrile and mechanical properties of its electrospun nanofibers. e-Polymers. 2018;18(6):569–73. doi: 10.1515/epoly-2018-0158.
(52) Zhao X, Yuan Y, Li P, Song Z, Ma C, Pan D, et al. A polyether amine modified metal organic framework enhanced the CO_2 adsorption capacity of room temperature porous liquids. Chem Comm. 2019;55(87):13179–82. doi: 10.1039/c9cc07243h.
(53) Song N, Sun Y, Xie X, Wang D, Shao F, Yu L, et al. Doping MIL-101(Cr)@GO in polyamide nanocomposite membranes with improved water flux. Desalination. 2020;492:114601. doi: 10.1016/j.desal.2020.114601.
(54) Yang P, Liu Q, Liu J, Zhang H, Li Z, Li R, et al. Interfacial growth of a metal-organic framework (UiO-66) on functionalized graphene oxide (GO) as a suitable seawater adsorbent for extraction of uranium(VI). J Mater Chem A. 2017;5(34):17933–42. doi: 10.1039/c6ta10022h.
(55) Liang Z, Wang J, Zhang Q, Zhuang T, Zhao C, Fu Y, et al. Composite PVDF ultrafiltration membrane tailored by sandwich-like GO@UiO-66 nanoparticles for breaking the trade-off between permeability and selectivity. Sep Purif Technol. 2021;276:119308. doi: 10.1016/j.seppur.2021.119308.